

# We are IntechOpen, the world's leading publisher of Open Access books Built by scientists, for scientists

6,900

Open access books available

186,000

International authors and editors

200M

Downloads

Our authors are among the

154

Countries delivered to

TOP 1%

most cited scientists

12.2%

Contributors from top 500 universities



WEB OF SCIENCE™

Selection of our books indexed in the Book Citation Index  
in Web of Science™ Core Collection (BKCI)

Interested in publishing with us?  
Contact [book.department@intechopen.com](mailto:book.department@intechopen.com)

Numbers displayed above are based on latest data collected.  
For more information visit [www.intechopen.com](http://www.intechopen.com)



---

# Ultrafast Intramolecular Proton Transfer Reaction of 1,2-Dihydroxyanthraquinone in the Excited State

---

Sebok Lee, Myungsam Jen, Kooknam Jeon,  
Jaebeom Lee, Joonwoo Kim and Yoonsoo Pang

Additional information is available at the end of the chapter

<http://dx.doi.org/10.5772/intechopen.75783>

---

## Abstract

1,2-Dihydroxyanthraquinone (alizarin) shows an ultrafast intramolecular proton transfer in the excited states between the adjacent hydroxyl and carbonyl groups. Due to the ground and electronic structure of locally excited and proton-transferred tautomers, alizarin shows dual emission bands with strong Stokes shifts. The energy barriers between the locally excited (LE) and proton-transferred (PT) tautomers in the excited state are strongly dependent on the solvent polarity and thus alizarin shows complicated photophysical properties including solvent and excitation dependences. The excited-state intramolecular proton transfer (ESIPT) of alizarin was monitored in time-resolved stimulated Raman spectroscopic investigation, where the instantaneous structural changes of anthraquinone backbone in 70~80 fs were captured. Two major vibrational modes of alizarin,  $\nu(\text{C}=\text{C})$  and  $\nu(\text{C}=\text{O})$  represent the proton transfer reaction in the excited state, which then leads to the vibrational relaxation of the product and the restructuring of solvent molecules. Ultrafast changes in solvent vibrational modes of dimethyl sulfoxide (DMSO) were also investigated for the solvation dynamics including hydrogen bond breaking and reformation.

**Keywords:** excited-state intramolecular proton transfer, tautomerization, femtosecond stimulated Raman, transient absorption

---

## 1. Introduction

Proton transfer occurring either intramolecularly or intermolecularly is one of the fundamental chemical reactions and has been of great interest in chemistry, biology, and related disciplines [1–5]. Molecules with the excited-state intramolecular proton transfer (ESIPT) often

show large Stokes shifts, which is beneficial in many photonic applications due to small self-absorption [6, 7]. The ESIPT reactions have been extensively studied by time-resolved spectroscopic methods, where the ultrafast laser pulses initiate the chemical reaction in the excited state [6–10]. Femtosecond transient absorption technique was used as the time-resolved electronic probe in monitoring ultrafast proton transfer reactions in the time scales of ~30 fs [8, 10]. Recently, a much faster ESIPT of ~13 fs in 10-hydroxybenzo[*h*]quinolone has been reported by a fluorescence upconversion technique [9].

1,2-Dihydroxyanthraquinone (alizarin) is one of natural red pigments which forms an intramolecular hydrogen bond between a carbonyl and a hydroxyl group in the ground and excited states [11–18]. Upon photoexcitation, a proton transfer from the hydroxyl to the carbonyl group occurs and the dual emission bands of the locally excited (LE) and proton-transferred (PT) tautomers have been reported [11–14]. The scheme of electronic structure of alizarin in LE and PT tautomers is shown in **Figure 1**. Since the barrier between LE and PT tautomers of alizarin in the excited state is tunable by changing solvent polarity [19, 20], the proton transfer reaction dynamics between the LE and PT tautomers might also be controlled by this factor. The emission band of the PT tautomer dominates in nonpolar aprotic solvents while the dual emission bands both from the LE and PT tautomers appear in polar aprotic solvents with the inhibition of the ESIPT reaction [21, 22]. According to the density functional theory (DFT)/time-dependent DFT (TDDFT) simulation results, the LE tautomer of alizarin is more stable (4.7–4.8 kcal/mol) than the PT tautomer in ground state, while the LE tautomer becomes

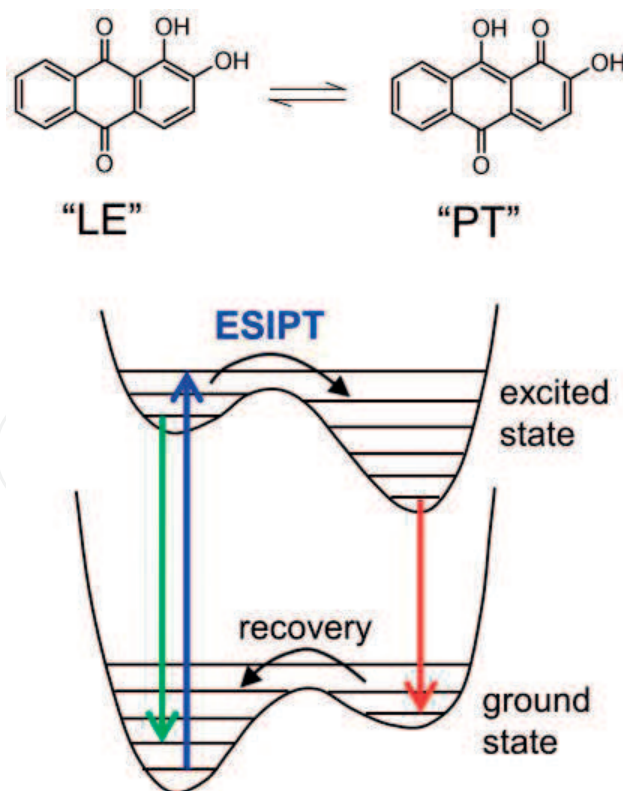


**Figure 1.** Electronic structure of alizarin in LE and PT tautomers. Adapted with permission from reference [41]. Copyright 2015 Elsevier.

less stable in the excited state with tunable energy barriers between the LE and PT [23]. For example, the energy barrier from the LE to PT tautomer in the excited state was estimated as 1.30 kcal/mol in benzene (nonpolar aprotic) and 3.19 kcal/mol in ethanol (polar aprotic).

The excited state lifetime of the alizarin PT tautomer was observed as 60–80 ps in several time-resolved spectroscopic investigations on alizarin, but the exact proton transfer dynamics of alizarin was not clearly obtained due to strong excited state absorption and emission signals, and complicated excited state dynamics including vibrational relaxations, solvations, etc., [20, 24–26]. However, the ultrafast ESIPT reactions (45–120 fs) of several anthraquinone derivatives including 1-hydroxyanthraquinone and 1-chloroacetylaminoanthraquinone have been measured by time-resolved fluorescent measurements [11, 15, 27, 28].

Femtosecond stimulated Raman spectroscopy (FSRS) with both high temporal (<50 fs) and spectral (<10 cm<sup>-1</sup>) resolutions was introduced recently for the study of excited state dynamics and reaction mechanisms [29, 30] and has been widely used to study the photo-induced population and structural dynamics in many chemical and biological systems [31–34].

In this chapter, the ESIPT reaction and excited state dynamics of alizarin will be overviewed by using experimental results of steady-state absorption and emission, femtosecond transient absorption, and femtosecond stimulated Raman measurement. The excited state dynamics of alizarin was examined by changing the solvent polarity and the evidence for the ultrafast proton transfer reaction and subsequent structural changes in the product state were inspected by the time-dependent skeletal vibrational modes of alizarin.

## 2. Experimental details

### 2.1. Chemical preparation

Alizarin (Sigma-Aldrich, St. Louis, MO), dimethyl sulfoxide (DMSO, Daejung Chemicals and Metals, Siheung, Korea), ethanol (Duksan Pure Chemicals, Ansan, Korea), and other chemicals were used as received. Alizarin hardly dissolves in water but dissolves in most organic solvents, so alizarin solutions (33–50 μM) were prepared in ethanol and DMSO for the steady-state absorption and emission, and transient absorption measurements. A 2 mm cell with a stirring magnet was used for transient absorption measurements to avoid photo-damage from the laser pulses. The DMSO solutions of alizarin up to 20-mM concentrations in a 0.5 mm flow cell recirculated by a peristaltic pump were used for stimulated Raman measurements.

### 2.2. Steady-state absorption and emission measurements

The absorption spectra were recorded by a UV/Vis spectrometer (S-3100, Scinco, Seoul, Korea) and the emission spectra were obtained by a time-resolved fluorescence setup based on a time-correlated single photon-counting module (PicoHarp 300, PicoQuant, Berlin, Germany), a picosecond diode laser ( $\lambda_{\text{ex}} = 405$  nm; P-C-405, PicoQuant), a monochromator (Cornerstone 260, Newport Corp., Irvine, CA), and a photomultiplier tube detector (PMA 192, PicoQuant).

### 2.3. Transient absorption spectroscopy

A femtosecond transient absorption setup based on a Ti:sapphire regenerative amplifier (LIBRA-USP-HE, Coherent Inc., Santa Clara, CA) was used for transient absorption measurements [35, 36]. The pump pulses at 403 nm were generated by sum-harmonic generation (SHG) in a BBO crystal ( $\theta = 29.2^\circ$ , Eksma Optics, Vilnius, Lithuania) and compressed in a prism-pair compressor. The whitelight supercontinuum probe pulses (450–1000 nm) generated in a sapphire window were tightly focused to the sample with the pump and detected with a fiber-based spectrometer (QE65Pro, Ocean Optics, Largo, FL). Transient absorption spectra and kinetics were analyzed in a global fit analysis by using a software package Glotaran [37].

### 2.4. Femtosecond stimulated Raman spectroscopy

A femtosecond stimulated Raman setup based on the Ti:sapphire regenerative amplifier (LIBRA-USP-HE) was used for time-resolved Raman measurements. A narrowband picosecond pulses (802 nm, 0.6 nm, 1.2 ps) generated by a home-built grating filter (1200 gr/mm) was used for the Raman pump, and a broadband (850–1000 nm) whitelight continuum generated in a YAG window (Newlight Photonics, Toronto, ON) was used for the Raman probe. The Raman probe filtered with long pass filters (FEL0850, Thorlabs Inc., Newton, NJ; 830 DCLP, Omega Optical Inc., Brattleboro, VT) was combined at the sample with the Raman pump and the actinic pump at 403 nm generated from SHG. The Raman pump was modulated at 500 Hz by an optical chopper (MC2000, Thorlabs Inc.) and the Raman probe was recorded at 1 kHz shot-to-shot level by a spectrograph (Triax 320, Horiba Jobin Yvon GmbH, Bensheim, Germany) and a CCD detector (PIXIS 100, Princeton Instruments, Trento, NJ). The optical time delay between the actinic pump and the Raman pump/probe pair was controlled by a motorized stage (MFN25PP, Newport Inc.) and a controller (ESP300, Newport Inc.). The Raman pump of 350 nJ pulse energy and the actinic pump of 750 nJ pulse energy were used in a typical FSRS measurement.

### 2.5. Computational details

DFT simulations for the Raman vibrational modes of alizarin were conducted by the Gaussian 09 software package (Gaussian Inc., Wallingford, CT), and the B3LYP/6-31G(d,p) level of theory with the optimized geometries from previous TDDFT results was used [23, 38]. The scaling factors for the vibrational frequencies obtained in previous reports were used to visualize the Raman spectra of alizarin both in ground and excited electronic states with arbitrary bandwidths of 10–15  $\text{cm}^{-1}$  [39].

## 3. Steady-state absorption and emission spectra of alizarin

In the ground state, the LE tautomer exists lower than the PT tautomer in energy and the energy barrier between two tautomers is too high for the proton transfer in the ground state to be observed [19]. On the other hand, the LE tautomer in the excited state which can be

approached by photoexcitation exists higher in energy than the PT tautomer, and the tautomerization to the PT tautomer can occur depending on the barrier height separating two tautomers [11–14, 16, 27, 40].

The absorption and emission spectra of alizarin in *n*-heptane, ethanol, and DMSO solution are shown in **Figure 2(a)**. The absorption spectrum of alizarin in *n*-heptane appears as several vibronic bands at ~405, 425, and 450 nm and the absorption bands of alizarin in both ethanol and DMSO are inhomogeneously broadened and red-shifted by 20–30 nm from the bands in *n*-heptane. The emission bands of alizarin in *n*-heptane centered at 610 and 660 nm show large Stokes' shifts from the absorption band representing the intramolecular proton transfer in the excited state. The emission spectra of alizarin in ethanol and DMSO show increased emission in the range of 500–600 nm in addition to main emission bands at 620 and 670 nm, which is interpreted as the emission signal originating from the LE state in the excited state.

**Figure 2(b)** shows the dependence of the excitation wavelength in the emission spectra of alizarin in ethanol. Alizarin shows two emission bands in ethanol solution. One centered at 535 nm from the LE tautomer appears strongly with 485 nm excitation, while the other centered at 620 nm from the PT tautomer becomes the main band with 405-nm excitation. The excess energy in the 405-nm excitation may facilitate the ESIPT by overcoming the energy barrier of the LE-PT tautomerization. Concentration and wavelength dependences in the emission spectra of alizarin can be the evidence for the existence of the energy barrier between the LE and PT tautomers [19, 20, 41].

To further investigate the intramolecular proton transfer of alizarin and the solvent dependence, the steady-state absorption and emission spectra of alizarin in binary mixtures of ethanol and water were measured with 405-nm excitation as shown in **Figure 3**. The absorption spectra of alizarin show a slight increase in absorbance with the addition of water to ethanol up to 50% without any spectral change. However, the emission spectra of alizarin show a strong solvent dependence. The PT emission bands at 615 and 670 nm decrease as the fraction of water increases up to 50% while the LE emission band at 530 nm increases. The isosbestic

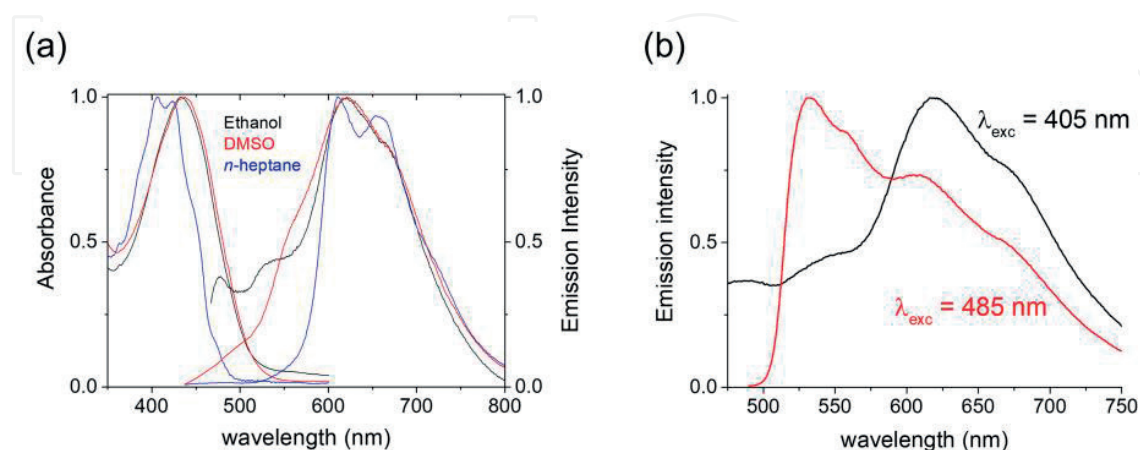


**Figure 2.** (a) Steady-state absorption and emission spectra of alizarin (adapted with permission from ref. [44]. Copyright 2017 ACS), (b) emission spectra of alizarin in ethanol with 405- and 485-nm excitations (adapted with permission from ref. [41]. Copyright 2015 Elsevier).

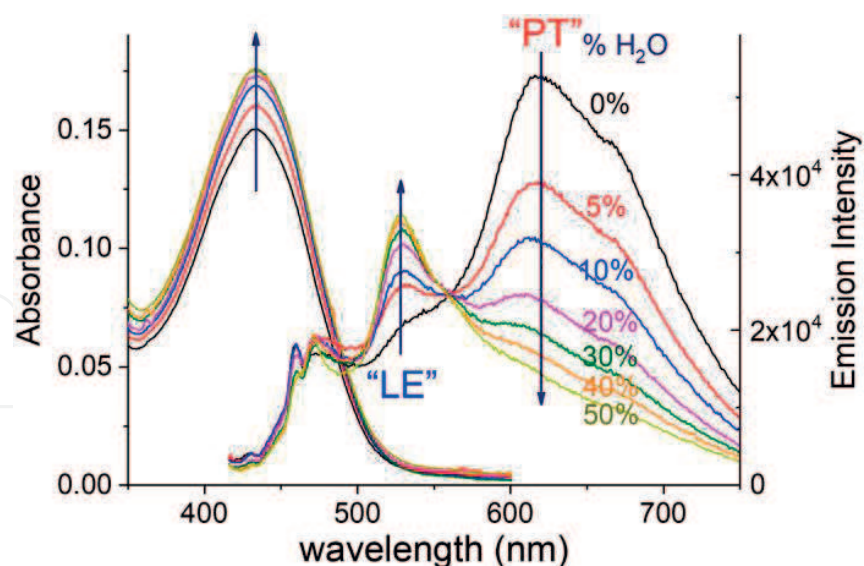


**Figure 3.** Steady-state absorption and emission spectra of alizarin in ethanol and binary mixtures of ethanol and water with 405-nm excitation. Adapted with permission from ref. [41]. Copyright 2015 Elsevier.

point between the LE and PT emission bands is clearly observed at 560 nm, which clearly supports the transition between the LE and PT tautomers. In addition, a decrease of overall quantum yield of alizarin with the addition of water may represent a nonradiative rate constant of the LE tautomer is much smaller than that of the PT tautomer. Recently, the effect of water on the ESIPT reaction of alizarin was further investigated by the simulations based on the time-dependent density functional theory [42]. It has been noted that the strong intramolecular hydrogen bonding of alizarin between the carbonyl and hydroxyl group may facilitate the ESIPT reaction in the excited state. Furthermore, the inhibition of the ESIPT process by water molecules by forming hydrogen bonds with the carbonyl or hydroxyl groups of alizarin was proposed, which weakens the intramolecular hydrogen bonding associated with the ESIPT process and thus increases the energy barrier between the LE and PT tautomer [42].

We have used time-resolved electronic (femtosecond transient absorption) and vibrational spectroscopy (FSRS) to further study the detailed kinetics and mechanism of the ESIPT reaction of alizarin in the excited state.

## 4. Excited state intramolecular proton transfer of alizarin

### 4.1. Femtosecond transient absorption results

Transient absorption results of alizarin in ethanol and in a binary mixture of ethanol:water = 1:1 with 403-nm excitation are shown in **Figure 4**. Within 10 ps time delay, the excited state absorption (ESA) band centered at 510 nm and the stimulated emission (SE) band in the 570–750 nm range are observed in both ethanol and ethanol-water mixture. A broad and weak ESA band in the 500–550 nm range is left after 1 ns time delay for the ethanol-water mixture, while all the excited state population of alizarin in ethanol solution decays to the ground state by the same

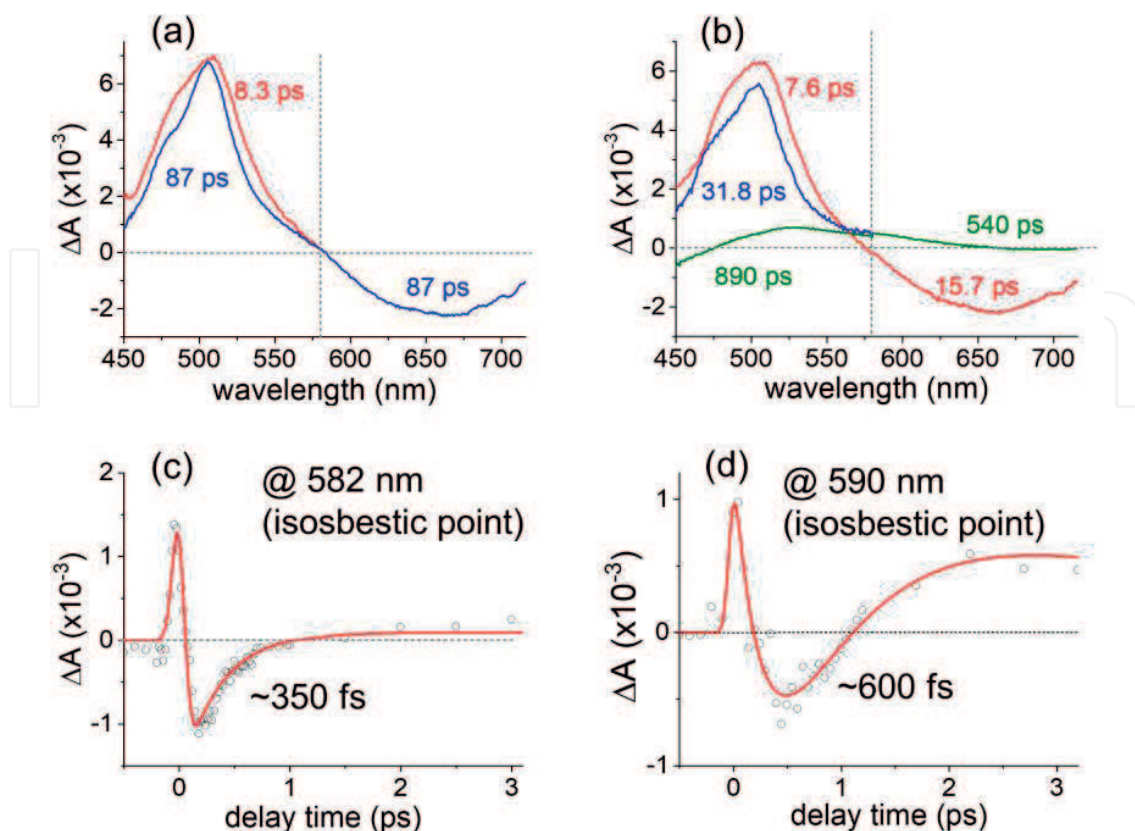


**Figure 4.** Transient absorption results of alizarin (a) in ethanol and (b) in 1:1 mixture of ethanol and water, excited-state kinetics of alizarin (c) in ethanol (582 nm) and (d) in DMSO (590 nm). Adapted from ref. [41]. Copyright 2015 Elsevier.

time. The global fit results for alizarin in ethanol are summarized by two kinetic components of 8.3 and 87 ps whose evolution associated difference spectra (EADS) are shown in **Figure 4(a)**. The 8.3 ps component with slightly broader absorption band (450–580 nm) but without emission signal represents the vibrationally hot PT tautomer, and the 87 ps component with both absorption and emission (580–750 nm) signals represents the relaxed PT tautomer in the excited state, which is consistent with previous results [20, 24–26].

The excited state dynamics of alizarin in ethanol-water mixture is somewhat complex. Instead of performing the global fit analysis of the whole transient absorption data, we analyzed the absorption (<580 nm) and emission (>580 nm) part of the data separately in the global fit analysis. We found three kinetic components of 7.6, 31.8, and 890 ps from the absorption part and two components of 15.7 and 540 ps from the emission part of the data. The kinetic components of 7.6 and 31.8 ps in the absorption part are tentatively assigned as the vibrationally hot and relaxed PT tautomers of alizarin, respectively, by inferring from the results of ethanol solution. However, the 7.6 ps component may include the decay of the LE state, as the blocking of the proton transfer reaction was observed with the addition of water from results of the steady-state emission spectra. The 15.7 ps lifetime of the first emission component of the data is much shorter than the lifetime of 31.8 ps component in the absorption part, thus this component may also represent the emission signal of both the LE and PT tautomer which cannot be separated in all the analysis we have done. In addition to the fast kinetic components for

the LE and PT tautomers, a long-lived component (540 or 890 ps) appeared as a very broad absorption band in 500–600 nm.

It is noted that the shortened lifetime of the PT tautomer (87 → 31.8 ps) with the addition of water to ethanol observed in transient absorption measurements is consistent to the reduced quantum yield and the increased nonradiative rate constant of alizarin observed in the steady-state emission measurements. As suggested by the recent theoretical study [42], water molecules may form hydrogen bonds with the carbonyl and hydroxyl groups of alizarin and impede the intramolecular proton transfer reaction of alizarin. Thus the long decay component in the transient absorption of alizarin in ethanol-water mixture may be considered as the “trapped” state of alizarin with water molecules. Further details on the solute-solvent interaction and resulting ESIPT kinetics can be investigated by FSRS, where time-resolved structural changes of solute and solvent molecules can be monitored.

It has been proposed that faster components of 300–400 fs time constant generally observed from the transient absorption signals of alizarin in the wavelengths (570–585 nm) where the strong ESA and SE signals cancel out, may represent the kinetics for the vibrational relaxation in the LE tautomer and the ESIPT to the PT tautomer [41, 43]. We also observed these fast components universally in the transient absorption results of alizarin in ethanol, methanol, DMSO, and ethanol-water mixture (examples are shown in **Figure 4(c)** and **(d)**), but did not show any dependence on the solvent polarity. Since the ESA, SE, and the ground-state bleaching signals of two tautomers of alizarin in transient absorption measurements are overlapped in wavelength and time, it seems to be very difficult to separate the kinetic components of the vibrational relaxation of the LE and PT tautomers, the ESIPT, etc. We conclude that the transient absorption measurements may be inadequate for the correct analysis of the ESIPT process, a further investigation by FSRS was performed to obtain the population and structural dynamics of alizarin upon photoexcitation.

## 4.2. Femtosecond stimulated Raman results

### 4.2.1. FSRS details

Alizarin is soluble in ethanol and DMSO but the Raman spectrum of ethanol overlaps that of alizarin in many spectral regions. Then small changes in the vibrational modes of alizarin might not be observed in ethanol solution due to strong Raman modes of ethanol. The Raman bands of DMSO, however, can be separable from the Raman modes of alizarin. Thus femtosecond stimulated Raman measurements of alizarin were done with DMSO solution. From the analysis of transient absorption result of alizarin in DMSO solution, two kinetic components were obtained [44]. Two components of 1.1 and 83.3 ps represent the vibrational relaxation in the PT tautomer and the lifetime of PT tautomer in the excited state, respectively. Although a fast (~600 fs) kinetic component was observed at 590 nm where the strong ESA and SE signals cancel out, it is not clear whether this component represents the ESIPT dynamics of alizarin.

The Raman intensity of the FSRS, often called the Raman gain can be evaluated by Eq. (1):

$$(\text{Raman Gain}) = \frac{I_{\text{R,Pump-ON}} - I_{\text{Bkg}}}{I_{\text{R,Pump-OFF}} - I_{\text{Bkg}}} \quad (1)$$

where  $I_{\text{R,Pump-ON}}$  and  $I_{\text{R,Pump-OFF}}$  represent the intensity of Raman probe with and without the Raman pump, respectively, and  $I_{\text{Bkg}}$  represents the dark signal of the CCD detector. The Raman probe

of 600,000 pulses (60 accumulations of 10-sec acquisition) was averaged in a typical Raman gain measurement with the half of them focused together with the Raman pump to the sample, to obtain a Raman gain signal in a signal-to-noise level of  $2 \times 10^{-5}$  (or 0.002%) at a specific time delay with the actinic pump pulses. Time-resolved stimulated Raman spectra of alizarin in DMSO at multiple time delays were obtained at time delays of  $-1$  to  $100$  ps and the ground state spectrum measured at  $-10$  ps time delay, for example, was subtracted from each stimulated Raman spectrum to obtain the difference stimulated Raman spectra shown in **Figure 5(a)**. A small portion of transient absorption signal, for example, the ESA and SE can be obtained together with stimulated Raman gain signals at most time delays, thus a polynomial background subtraction was performed to remove the transient absorption signal.

#### 4.2.2. The population and structural dynamics of the ESIPT

Major Raman bands of the ground electronic state of alizarin in the  $1500$ – $1800$   $\text{cm}^{-1}$  range shown in **Figure 5(a)** were assigned as the ring  $\nu(\text{C}=\text{C})$  at  $1573$  and  $1594$   $\text{cm}^{-1}$ , and  $\nu(\text{C}=\text{O})$  at  $1634$  and  $1661$   $\text{cm}^{-1}$  mainly according to the DFT simulation results. One  $\nu(\text{C}=\text{O})$  at  $1661$   $\text{cm}^{-1}$  is assigned to the isolated carbonyl at C10 position and the other at  $1634$   $\text{cm}^{-1}$  is the carbonyl at the site of the ESIPT and adjacent to a hydroxyl group [44]. Another Raman band at  $1191$   $\text{cm}^{-1}$  is assigned as  $\delta(\text{CH})$  and  $\delta(\text{OH})$ . In the excited stimulated Raman spectra of alizarin, several Raman bands at  $1162$ ,  $1555$ , and  $1632$   $\text{cm}^{-1}$  appeared in  $50$ – $100$  fs after the photoexcitation and showed a decay after  $20$  ps or so. According to the TDDFT simulation results [23, 44], we tentatively assign the  $1162$   $\text{cm}^{-1}$  band as the  $\delta(\text{CH})$  and  $\delta(\text{OH})$  of the PT tautomer, and the  $1555$  and  $1632$   $\text{cm}^{-1}$  as  $\nu(\text{C}=\text{C})$  and  $\nu(\text{C}=\text{O})$  bands also in the PT tautomer of alizarin.

To obtain the details of the excited state dynamics and the ESIPT from the stimulated Raman bands of alizarin, the experimental data were fit with a low-order polynomial background and several Gaussian functions for Raman bands. The population dynamics of  $\nu(\text{C}=\text{C})$  and  $\nu(\text{C}=\text{O})$  bands at  $1555$  and  $1632$   $\text{cm}^{-1}$  shown in **Figure 5(b)** shows a ubiquitous sharp rise in  $70$ – $80$  fs and a slow decay into the ground state which is compatible to the PT tautomer's lifetime of  $83.3$  ps as shown in the transient absorption results. The structural dynamics of  $\nu(\text{C}=\text{C})$  and  $\nu(\text{C}=\text{O})$  modes of the PT tautomer are shown in **Figure 5(c)** and **(d)** as the time-dependent changes in the peak position and the bandwidth. The peak shift of the solvent vibrational mode,  $\delta(\text{CH}_3)$  of DMSO at  $1421$   $\text{cm}^{-1}$  represents the instrument response function of FSRS measurements for comparison with the excited dynamics of alizarin Raman bands. It is interesting to note that a strong blue-shift ( $1540 \rightarrow 1553$   $\text{cm}^{-1}$ ) and a decrease of bandwidth ( $28 \rightarrow 24$   $\text{cm}^{-1}$ ) of  $\nu(\text{C}=\text{C})$  band all occur in an ultrafast time scale of  $\sim 150$  fs after photoexcitation. On the other hand, the  $\nu(\text{C}=\text{O})$  band shows a strong red-shift ( $1645 \rightarrow 1630$   $\text{cm}^{-1}$ ) in the same time delay of  $100$ – $150$  fs although this vibrational band appears too broad for the bandwidth analysis. As well represented in **Figure 5(b–d)**, the population growth and the structural changes of  $\nu(\text{C}=\text{C})$  and  $\nu(\text{C}=\text{O})$  Raman bands of the PT tautomer of alizarin are interpreted as the ESIPT process from the LE to the PT tautomer. Since no Raman band of the LE tautomer has been identified from the FSRS results, this could also be included for the dynamics of  $\nu(\text{C}=\text{C})$  and  $\nu(\text{C}=\text{O})$  bands at  $1555$  and  $1632$   $\text{cm}^{-1}$ . The vibrational relaxation along an electronic potential surface would generally result in slight blue-shifts in the strongly coupled vibrational modes due to the anharmonicity of the electric potential surface. However, the  $\nu(\text{C}=\text{C})$  and  $\nu(\text{C}=\text{O})$  bands showed strong ( $\sim 15$   $\text{cm}^{-1}$ ) peak shifts either in increasing and decreasing bandwidth, respectively, during the ultrafast period of the population growth for the PT tautomer. This cannot be explained by any type of relaxation inside the same

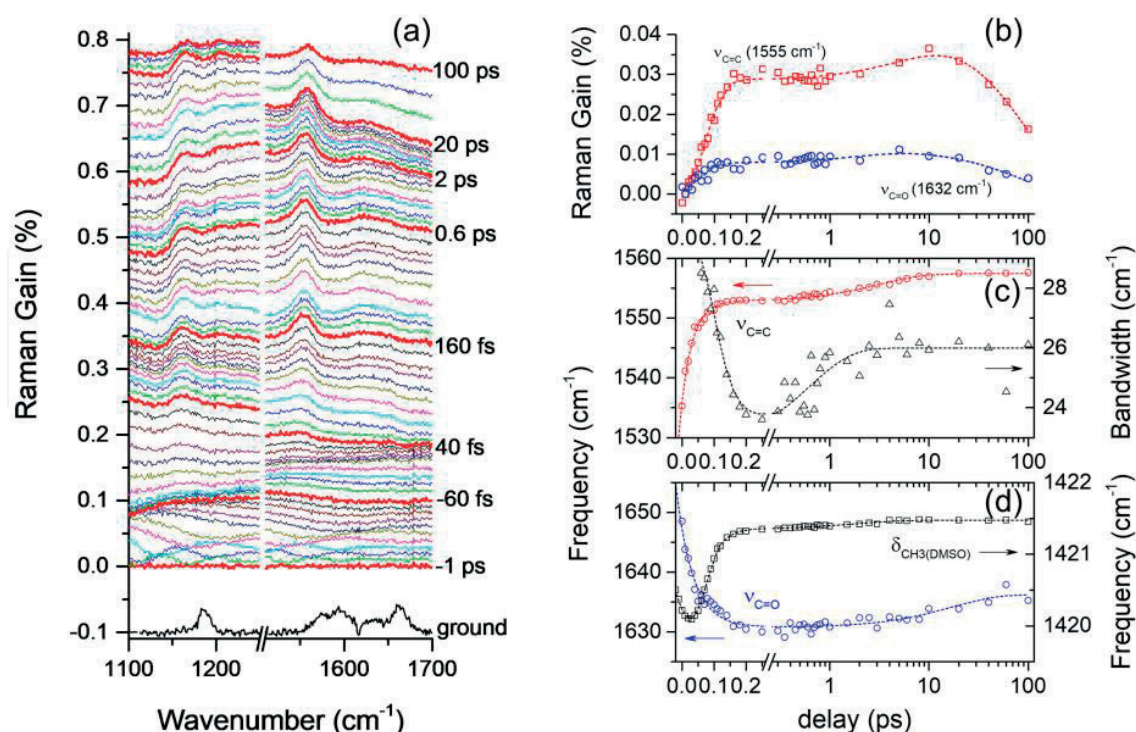


**Figure 5.** (a) Time-resolved stimulated Raman spectra of alizarin in DMSO following 403-nm photoexcitation, (b) population dynamics for the Raman bands of  $\nu(\text{C}=\text{C})$  at  $1555\text{ cm}^{-1}$  and  $\nu(\text{C}=\text{O})$  at  $1632\text{ cm}^{-1}$ , (c)  $\nu(\text{C}=\text{C})$  and (d)  $\nu(\text{C}=\text{O})$  Raman bands from the PT conformer of alizarin in the excited state and peak shift of a solvent  $\delta(\text{CH}_3)$  mode which represents the instrument response function of FSRs measurements. Adapted with permission from ref. [44]. Copyright 2017 ACS.

potential surface but has to be understood as the nuclear rearrangements for the intramolecular proton transfer reaction. Therefore, we conclude that the intramolecular proton transfer reaction of alizarin in the excited state occurs in ultrafast time scale of 70–80 fs.

Another interesting fact is the strong and opposite peak shifts observed for  $\nu(\text{C}=\text{C})$  and  $\nu(\text{C}=\text{O})$  bands during the ESIPT reaction. We could imagine a transition state for the ESIPT reaction of alizarin as a six-membered ring formed by intramolecular hydrogen bonding between carbonyl group and hydroxyl group. We propose that the strong and opposite peak shifts of the  $\nu(\text{C}=\text{C})$  and  $\nu(\text{C}=\text{O})$  band directly represent the changes in the resonance structure of the alizarin backbone which is composed of multiple C=C and C-C bonds and a C=O. The details of the ESIPT reaction mechanism of alizarin need be confirmed by thorough theoretical investigations, which is beyond of the scope of this chapter. The reaction mechanism of many ESIPT reactions and the existence of transition states have been recently reported by several theoretical works based on TDDFT and several transition states of six-membered ring between carbonyl and hydroxyl groups were represented for 1,8-dihydroxy-2-naphthaldehyde [7, 45, 46]. Although a separate transition state of the ESIPT reaction was not resolved from the FSRs results, we also propose the reaction may occur via the transition state of a new hydrogen-bond six-membered ring attached to the anthraquinone backbone.

As shown in **Figure 5(b–d)**, two more kinetic components other than the population decay of the PT tautomer were identified. A slight blue-shift ( $1553 \rightarrow 1557\text{ cm}^{-1}$ ) and an increased bandwidth ( $24 \rightarrow 26\text{ cm}^{-1}$ ) of  $\nu(\text{C}=\text{C})$  mode observed in 3–10 ps and another slight blue-shift

(1630  $\rightarrow$  1636  $\text{cm}^{-1}$ ) of  $\nu(\text{C}=\text{O})$  mode shown in 20–30 ps represent the vibrational relaxation in the product potential surface of the PT conformer. There were no further changes in peak position and bandwidth of  $\nu(\text{C}=\text{C})$  and  $\nu(\text{C}=\text{O})$  modes during the population decay of the PT tautomer, which also supports the assignment of the vibrational relaxation in the PT potential surface.

## 5. Solvation dynamics

The intramolecular proton transfer reaction of alizarin in the excited state was evidenced by the population and structural dynamics of two major vibrational modes of  $\nu(\text{C}=\text{C})$  and  $\nu(\text{C}=\text{O})$ . Ultrafast ESIPT reaction of alizarin in the excited state can also be observed indirectly by the changes in the solvent vibrational spectrum such as the instantaneous disruption of the solvation shells and the formation of new solvation. **Figure 6(a)** and **(b)** show the difference stimulated Raman spectra of the solvent DMSO, especially  $\nu(\text{S}=\text{O})$  at 1044  $\text{cm}^{-1}$  with alizarin concentrations of 20 and 1 mM, respectively. Solvent DMSO is known to form hydrogen bonds in solution between S=O and C-H groups, and also a polymeric structure is formed at low temperature [47]. The Raman band of  $\nu(\text{S}=\text{O})$  is composed of multiple subbands including the symmetric (1026  $\text{cm}^{-1}$ ) and antisymmetric stretching (1042  $\text{cm}^{-1}$ ) of dimer, the symmetric stretching (1058  $\text{cm}^{-1}$ ) of monomer, etc., [47, 48]. In the DMSO solutions of alizarin in 0–15 mM concentration range, the  $\nu(\text{S}=\text{O})$  band of DMSO shows strong peak shifts (1042  $\rightarrow$  1024  $\text{cm}^{-1}$ ), which represents changes in the hydrogen bonding network of DMSO [44]. The  $\delta(\text{CH}_3)$  band of DMSO shows no major spectral changes upon the alizarin concentration, thus the solvation of alizarin with DMSO mainly occurs via hydrogen bonds with the sulfoxide group of DMSO [44].

As shown in **Figure 6(a)** and **(b)**, a sharp dispersive pattern in the  $\nu(\text{S}=\text{O})$  band appears instantly with the actinic pulse for both 20 and 1 mM concentrations of alizarin. The Raman intensity for the symmetric stretching of monomer around 1060  $\text{cm}^{-1}$  decreases and the symmetric stretching of dimer around 1025  $\text{cm}^{-1}$  increases, which clearly shows the instantaneous changes in hydrogen bonding of DMSO molecules. As clearly seen with the 1-mM solution case, this dispersive pattern disappears very quickly as the actinic pulse leaves the solution. In other words, a disruption in the hydrogen bonding of DMSO molecules created by ultrafast laser pulses is removed quickly by reforming hydrogen bonds between DMSO molecules. It seems that the hydrogen bond reformation occurs much faster than the instrument response function of FSRS ( $\sim$ 100 fs). Considering from the ultrafast dynamics of the dispersive signals of  $\nu(\text{S}=\text{O})$  band, the nonpolar solvation effect may be understood as the origin of this sharp dispersive signal [49–51]. We have also observed a similar dispersive background signal in the  $\delta(\text{CH}_3)$  band of DMSO [44].

On the other hand, the 20-mM alizarin results showed clearly distinct dynamics for the  $\nu(\text{S}=\text{O})$  band as shown in **Figure 6(a)**. The initial dispersive Raman signals were almost removed in about 100 fs then another type of dispersive Raman signals appeared, which is composed of a small bleaching with almost the same spectral shape as the ground state  $\nu(\text{S}=\text{O})$  band and a much broader positive signal around 990  $\text{cm}^{-1}$ . **Figure 7** clearly shows this dispersive Raman pattern in the  $\nu(\text{S}=\text{O})$  of DMSO appearing 100 fs after the actinic pump, where the initial dispersive Raman signals of the  $\nu(\text{S}=\text{O})$  obtained with 1-mM alizarin solution were subtracted from the results with 20-mM alizarin solution. The bleaching of the ground state  $\nu(\text{S}=\text{O})$  Raman band may result from the local heating due to the vibrational cooling of solute molecules, then the recovery of the

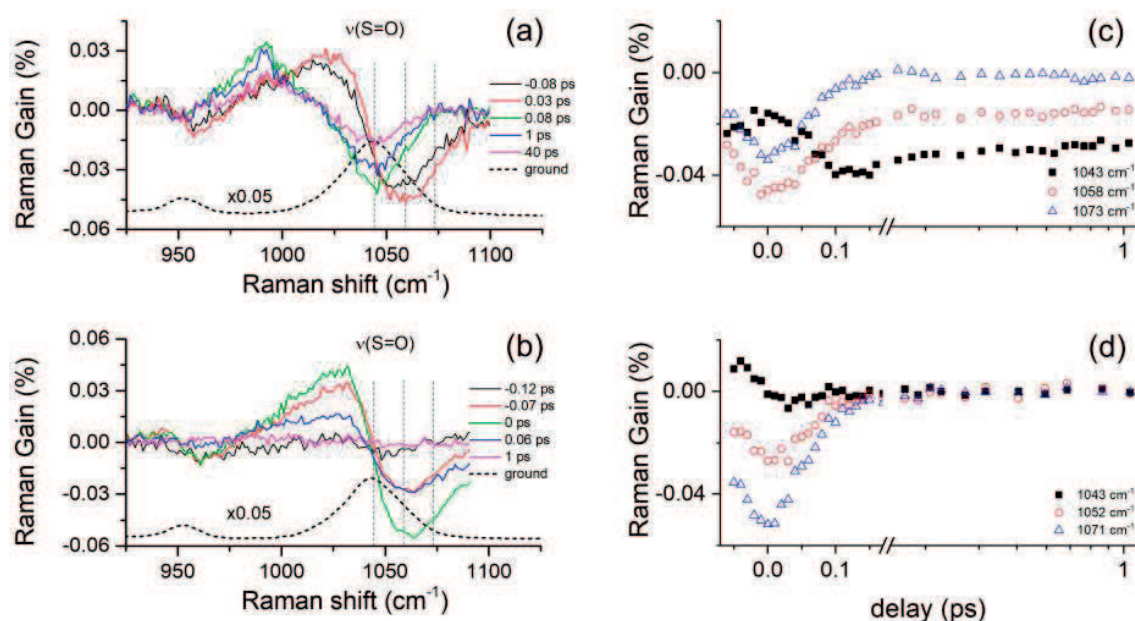


**Figure 6.** Difference stimulated Raman spectra of  $\nu(\text{S}=\text{O})$  mode of DMSO in (a) 20- and (b) 1-mM alizarin solution, the excited-state kinetics of  $\nu(\text{S}=\text{O})$  bands at several frequencies in (c) 20- and (d) 1-mM alizarin solution. Adapted from ref. [44]. Copyright 2017 ACS.

bleaching signals by the local cooling would take several tens of picoseconds [51–53]. The decay of the second dispersive Raman signals at 990 and 1043  $\text{cm}^{-1}$  is compatible to the local cooling time but a huge frequency difference ( $\sim 50 \text{ cm}^{-1}$ ) cannot be explained by the local heating of solvent DMSO. In a control experiment to measure temperature-dependent Raman spectra for the  $\nu(\text{S}=\text{O})$  of DMSO, the spectral changes of less than 5  $\text{cm}^{-1}$  were observed with temperature increase of 40–50  $^{\circ}\text{C}$ . Therefore, we conclude that the second dispersive Raman signals of  $\nu(\text{S}=\text{O})$  appearing at 100 fs time delay and between 990 and 1043  $\text{cm}^{-1}$  cannot be explained as the local heating of solvent molecules pumped by vibrationally cooled solute molecules and the changes in the solvation

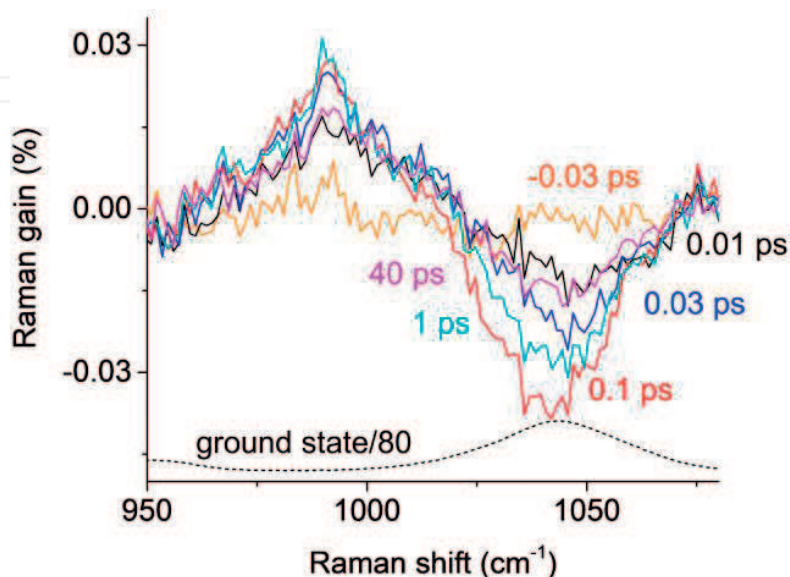


**Figure 7.** Dispersive Raman signals of  $\nu(\text{S}=\text{O})$  of DMSO. The initial dispersive pattern due to nonpolar solvation changes of DMSO molecules is subtracted.

shells of DMSO molecules due to the ESIPT reaction of alizarin molecules from the LE to the PT tautomers must be considered. Different from the initial dispersive signals in the  $\nu(\text{S}=\text{O})$  and  $\delta(\text{CH}_3)$  bands of DMSO, the second dispersive signals in the  $\nu(\text{S}=\text{O})$  must be considered as originating from the polar or dielectric type of solvation [51]. The dispersive Raman signal of the  $\nu(\text{S}=\text{O})$  band at  $1044\text{ cm}^{-1}$  showed a growth with a  $60 \pm 30\text{ fs}$  time constant and a decay with a  $4.9 \pm 1.5\text{ ps}$  time constant, which clearly shows that the hydrogen-bonding network of DMSO was created by the ESIPT reaction of alizarin and decayed as the vibrational relaxation of the product along the potential surface of the PT tautomer in the excited state. In this work, we showed that the  $\nu(\text{S}=\text{O})$  band of solvent DMSO can be used to determine the ultrafast ESIPT reaction and the subsequent vibrational relaxation in the reaction product. The breaking and reforming of hydrogen-bonding network of DMSO can be successfully observed by the  $\nu(\text{S}=\text{O})$  band of DMSO thus this method can also be applied to many chemical reactions occurring in the photoinduced excited states.

## 6. Conclusion

In this chapter, the ESIPT reaction and the excited state dynamics of alizarin were explored by time-resolved electronic and vibrational spectroscopy with the femtosecond time-resolution. The dependence on solvent polarity and excitation wavelength was observed in the steady-state emission spectra of alizarin, where the barrier height between the LE and PT tautomers in the excited state may exist and be controlled by the solvent polarity. The transient absorption results of alizarin in ethanol and ethanol-water mixture were so complicated and overlapping, so the ESIPT rate constant from the LE to the PT tautomers was not separable from the vibrational relaxation and population decay of both tautomers. Instead, the ESIPT of alizarin in the excited state was clearly observed in femtosecond stimulated Raman measurements. The population and structural dynamics of two major vibrational modes of  $\nu(\text{C}=\text{C})$  and  $\nu(\text{C}=\text{O})$  clearly showed the dynamics of the ESIPT rate to the PT tautomer, the vibrational relaxation and the population decay of the product PT tautomer. The vibrational signature of the LE tautomer was not observed in FSRS, but the reaction mechanism of the ESIPT including a transition state of a newly formed six-membered ring composed of the carbonyl and hydroxyl groups was estimated by the strong and opposite peak shifts of  $\nu(\text{C}=\text{C})$  and  $\nu(\text{C}=\text{O})$  seen in the stimulated Raman spectra of alizarin during the reaction. From the population growth and structural transformation into the PT tautomer, we concluded that the ESIPT of alizarin occurs in an ultrafast time scale of 70–80 fs. During the ESIPT reaction of alizarin, solvent DMSO molecules showed ultrafast structural changes involving hydrogen bonds with solute molecules. When the solute concentration is very low, DMSO shows a dispersive Raman signal in the  $\nu(\text{S}=\text{O})$  and  $\delta(\text{CH}_3)$  modes only with the actinic pump. The instantaneous disruption and reformation of hydrogen bonds may suggest a nonpolar type of solvation between solvent molecules. On the other hand, complicated dispersive Raman signals in the  $\nu(\text{S}=\text{O})$  mode of DMSO were observed with a concentrated (20 mM) solution of alizarin. After the same instantaneous solvent responses completed in 100 fs, the second dispersive Raman pattern with a bleaching of the ground state spectrum appeared and decayed with 60 fs and 5 ps time scales. This also represents the disruption of hydrogen bonds of DMSO molecules, more specifically between solute molecules and in the polar or dielectric solvation shells. Interestingly, the dynamics for the ultrafast proton transfer reaction and the vibrational relaxation in the product state was measured by the solvation signals of solvent DMSO.

## Acknowledgements

This work was supported by Basic Science Research Program funded by the Ministry of Education (2017R1A1D1B03027870, 2014R1A1A2058409) and by the International Cooperation Program (2016K2A9A1A01951845), through the National Research Foundation of Korea (NRF). The GIST Research Institute (GRI) in 2018 and the PLSI supercomputing resources of the Korea Institute of Science and Technology Information also supported this research.

## Conflict of interest

The authors declare no conflict of interest.

## Author details

Sebok Lee<sup>1†</sup>, Myungsam Jen<sup>1†</sup>, Kooknam Jeon<sup>1</sup>, Jaebeom Lee<sup>2</sup>, Joonwoo Kim<sup>1</sup> and Yoonsoo Pang<sup>1\*</sup>

\*Address all correspondence to: ypang@gist.ac.kr

1 Department of Chemistry, Gwangju Institute of Science and Technology, Gwangju, Republic of Korea

2 Department of Physics and Photon Science, Gwangju Institute of Science and Technology, Gwangju, Republic of Korea

<sup>†</sup>These authors contributed equally

## References

- [1] Rini M, Magnes BZ, Pines E, Nibbering ETJ. Real-time observation of bimodal proton transfer in acid-base pairs in water. *Science*. 2003;**301**:349-352. DOI: 10.1126/science.1085762
- [2] Siwick BJ, Cox MJ, Bakker HJ. Long-range proton transfer in aqueous acid-base reactions. *Journal of Physical Chemistry B*. 2008;**112**:378-389. DOI: 10.1021/jp075663i
- [3] Perez-Lustres JL, Rodriguez-Prieto F, Mosquera M, Senyushkina TA, Ernstring NP, Kovalenko SA. Ultrafast proton transfer to solvent: Molecularity and intermediates from solvation- and diffusion-controlled regimes. *Journal of the American Chemical Society*. 2007;**129**:5408-5418. DOI: 10.1021/ja0664990
- [4] Elsaesser T, Kaiser W, Luettker W, Luttker W. Picosecond spectroscopy of intramolecular hydrogen bonds in 4,4',7,7'-Tetramethylindigo. *Journal of Physical Chemistry*. 1986;**90**:2901-2905. DOI: 10.1021/j100404a024

- [5] Ernsting NP. Dual fluorescence and excited-state intramolecular proton transfer in jet-cooled 2,5-Bis(2-benzoxazolyl) hydroquinone. *Journal of Physical Chemistry*. 1985;**89**:4932-4939. DOI: 10.1021/j100269a010
- [6] Simkovitch R, Huppert D. Excited-state intramolecular proton transfer of the natural product quercetin. *Journal of Physical Chemistry B*. 2015;**119**:10244-10251. DOI: 10.1021/acs.jpcc.5b04867
- [7] Tseng HW, Liu JQ, Chen YA, Chao CM, Liu KM, Chen CL, et al. Harnessing excited-state intramolecular proton-transfer reaction via a series of amino-type hydrogen-bonding molecules. *Journal of Physical Chemistry Letters*. 2015;**6**:1477-1486. DOI: 10.1021/acs.jpcclett.5b00423
- [8] Takeuchi S, Tahara T. Coherent nuclear wavepacket motions in ultrafast excited-state intramolecular proton transfer: Sub-30-fs resolved pump-probe absorption spectroscopy of 10-hydroxybenzo[h]quinoline in solution. *Journal of Physical Chemistry A*. 2005;**109**:10199-10207. DOI: 10.1021/jp0519013
- [9] Kim CH, Joo T. Coherent excited state intramolecular proton transfer probed by time-resolved fluorescence. *Physical Chemistry Chemical Physics*. 2009;**11**:10266-10269. DOI: 10.1039/b915768a
- [10] Lochbrunner S, Wurzer AJ, Riedle E. Microscopic mechanism of ultrafast excited-state intramolecular proton transfer: A 30-fs study of 2-(2'-hydroxyphenyl)benzothiazole. *Journal of Physical Chemistry A*. 2003;**107**:10580-10590. DOI: 10.1021/jp035203z
- [11] Flom SR, Barbara PF. Proton transfer and hydrogen bonding in the internal conversion of S1 Anthraquinones. *Journal of Physical Chemistry*. 1985;**89**:4489-4494. DOI: 10.1021/j100267a017
- [12] Miliani C, Romani A, Favaro G. Acidichromic effects in 1,2-di- and 1,2,4-trihydroxyanthraquinones. A spectrophotometric and fluorimetric study. *Journal of Physical Organic Chemistry*. 2000;**13**:141-150. DOI: 10.1002/(SICI)1099-1395(200003)13:3
- [13] Mech J, Grela M, Szaciłowski K. Ground and excited state properties of alizarin and its isomers. *Dyes and Pigments*. 2014;**103**:202-213. DOI: 10.1016/j.dyepig.2013.12.009
- [14] Le Person A, Cornard JP, Say-Liang-Fat S. Studies of the tautomeric forms of alizarin in the ground state by electronic spectroscopy combined with quantum chemical calculations. *Chemical Physics Letters*. 2011;**517**:41-45. DOI: 10.1016/j.cplett.2011.10.015
- [15] Neuwahl FVR, Bussotti L, Righini R, Buntinx G. Ultrafast proton transfer in the S1 state of 1-chloroacetylaminoanthraquinone. *Physical Chemistry Chemical Physics*. 2001;**3**:1277-1283. DOI: 10.1039/b007312l
- [16] Cho SH, Huh H, Kim HM, Kim NJ, Kim SK. Infrared-visible and visible-visible double resonance spectroscopy of 1-hydroxy-9,10-anthraquinone-(H<sub>2</sub>O)<sub>n</sub> (n=1,2) complexes. *Journal of Chemical Physics*. 2005;**122**:34305. DOI: 10.1063/1.1829991
- [17] Habeeb MM, Alghanmi RM. Spectrophotometric study of intermolecular hydrogen bonds and proton transfer complexes between 1,2-dihydroxyanthraquinone and some

- aliphatic amines in methanol and acetonitrile. *Journal of Chemical & Engineering Data*. 2010;**55**:930-936. DOI: 10.1021/jc900528h
- [18] Cysewski P, Jeliński T, Przybyłek M, Shyichuk A. Color prediction from first principle quantum chemistry computations: A case of alizarin dissolved in methanol. *New Journal of Chemistry*. 2012;**36**:1836-1843. DOI: 10.1039/c2nj40327g
- [19] Sasirekha V, Umadevi M, Ramakrishnan V. Solvatochromic study of 1,2-dihydroxyanthraquinone in neat and binary solvent mixtures. *Spectrochimica Acta - Part A: Molecular and Biomolecular Spectroscopy*. 2008;**69**:148-155. DOI: 10.1016/j.saa.2007.03.021
- [20] Reta MR, Anunziata JD, Cattana RI, Silber JJ. Comparison between solvatochromic and chromatographic studies of anthraquinones in binary aqueous mixtures. *Analytica Chimica Acta*. 1995;**306**:81-89. DOI: 10.1016/0003-2670(94)00595-D
- [21] Zhao J, Ji S, Chen Y, Guo H, Yang P. Excited state intramolecular proton transfer (ESIPT): From principal photophysics to the development of new chromophores and applications in fluorescent molecular probes and luminescent materials. *Physical Chemistry Chemical Physics*. 2012;**14**:8803-8817. DOI: 10.1039/C2CP23144A
- [22] Kwon JE, Park SY. Advanced organic optoelectronic materials: Harnessing excited-state intramolecular proton transfer (ESIPT) process. *Advanced Materials*. 2011;**23**:3615-3642. DOI: 10.1002/adma.201102046
- [23] Amat A, Miliani C, Romani A, Fantacci S. DFT/TDDFT investigation on the UV-vis absorption and fluorescence properties of alizarin dye. *Physical Chemistry Chemical Physics*. 2015;**17**:6374-6382. DOI: 10.1039/c4cp04728a
- [24] Dworak L, Matylitsky VV, Wachtveitl J. Ultrafast photoinduced processes in alizarin-sensitized metal oxide mesoporous films. *ChemPhysChem*. 2009;**10**:384-391. DOI: 10.1002/cphc.200800533
- [25] Matylitsky VV, Lenz MO, Wachtveitl J. Observation of pH-dependent back-electron-transfer dynamics in alizarin/TiO<sub>2</sub> adsorbates: Importance of trap states. *Journal of Physical Chemistry B*. 2006;**110**:8372-8379. DOI: 10.1021/jp060588h
- [26] Huber R, Moser J, Gratzel M, Wachtveitl J. Real-time observation of photoinduced adiabatic Electron transfer in strongly coupled dye/semiconductor colloidal systems with a 6 fs time constant. *Journal of Physical Chemistry B*. 2002;**106**:6494-6499. DOI: 10.1021/jp0155819
- [27] Choi JR, Jeoung SC, Cho DW. Two-photon-induced excited-state intramolecular proton transfer process in 1-hydroxyanthraquinone. *Chemical Physics Letters*. 2004;**385**:384-388. DOI: 10.1016/j.cplett.2004.01.011
- [28] Ryu J, Woo Kim H, Soo Kim M, Joo T. Ultrafast excited state intramolecular proton transfer dynamics of 1-hydroxyanthraquinone in solution. *Bulletin of the Korean Chemical Society*. 2013;**34**:465-469. DOI: 10.5012/bkcs.2013.34.2.465

- [29] Zhu L, Liu W, Fang C. A versatile femtosecond stimulated Raman spectroscopy setup with tunable pulses in the visible to near infrared. *Applied Physics Letters*. 2014;**105**:41106. DOI: 10.1063/1.4891766
- [30] Kovalenko SA, Dobryakov AL, Ernsting NP. An efficient setup for femtosecond stimulated Raman spectroscopy. *Review of Scientific Instruments*. 2011;**82**:63102. DOI: 10.1063/1.3596453
- [31] Kukura P, McCamant DW, Mathies RA. Femtosecond stimulated Raman spectroscopy. *Annual Review of Physical Chemistry*. 2007;**58**:461-488. DOI: 10.1146/annurev.physchem.58.032806.104456
- [32] McAnally MO, McMahon JM, Van Duyne RP, Schatz GC. Coupled wave equations theory of surface-enhanced femtosecond stimulated Raman scattering. *Journal of Chemical Physics*. 2016;**145**:94106. DOI: 10.1063/1.4961749
- [33] Hoffman DP, Mathies RA. Femtosecond stimulated Raman exposes the role of vibrational coherence in condensed-phase photoreactivity. *Accounts of Chemical Research*. 2016;**49**:616-625. DOI: 10.1021/acs.accounts.5b00508
- [34] Frontiera RR, Mathies RA. Femtosecond stimulated Raman spectroscopy. *Laser & Photonics Reviews*. 2011;**5**:102-113. DOI: 10.1002/lpor.200900048
- [35] Lee I, Lee S, Pang Y. Excited-state dynamics of carotenoids studied by femtosecond transient absorption spectroscopy. *Bulletin of the Korean Chemical Society*. 2014;**35**:851-857. DOI: 10.5012/bkcs.2014.35.3.851
- [36] Jen M, Lee S, Pang Y. Excited-state dynamics of all-trans-retinal investigated by time-resolved electronic and vibrational spectroscopy. *Bulletin of the Korean Chemical Society*. 2015;**36**:900-905. DOI: 10.1002/bkcs.10168
- [37] Van Stokkum IHM, Larsen DS, Van Grondelle R. Global and target analysis of time-resolved spectra. *Biochimica et Biophysica Acta, Bioenergetics*. 2004;**1657**:82-104. DOI: 10.1016/j.bbabi.2004.04.011
- [38] Frisch MJ, Trucks GW, Schlegel HB, Scuseria GE, Robb MA, Cheeseman JR, et al. *Gaussian 09, Revision A.02*. Wallingford CT: Gaussian, Inc; 2009
- [39] Irikura KK, Johnson RD, Kacker RN. Uncertainties in scaling factors for ab initio vibrational frequencies. *Journal of Physical Chemistry A*. 2005;**109**:8430-8437. DOI: 10.1021/jp052793n
- [40] Smith TP, Zaklika KA, Thakur K, Walker GC, Tominaga K, Barbara PF. Spectroscopic studies of excited-state intramolecular proton-transfer in 1-(acylamino)anthraquinones. *Journal of Physical Chemistry*. 1991;**95**:10465-10475. DOI: 10.1021/j100178a038
- [41] Lee S, Lee J, Pang Y. Excited state intramolecular proton transfer of 1,2-dihydroxyanthraquinone by femtosecond transient absorption spectroscopy. *Current Applied Physics*. 2015;**15**:1492-1499. DOI: 10.1016/j.cap.2015.08.017

- [42] Peng Y, Ye Y, Xiu X, Sun S. Mechanism of excited-state intramolecular proton transfer for 1,2-dihydroxyanthraquinone: Effect of water on the ESIPT. *Journal of Physical Chemistry A*. 2017;**121**:5625-5634. DOI: 10.1021/acs.jpca.7b03877
- [43] Huber R, Spörlein S, Moser JE, Grätzel M, Wachtveitl J. The role of surface states in the ultrafast photoinduced electron transfer from sensitizing dye molecules to semiconductor colloids. *Journal of Physical Chemistry B*. 2000;**104**:8995-9003. DOI: 10.1021/jp9944381
- [44] Jen M, Lee S, Jeon K, Hussain S, Pang Y. Ultrafast intramolecular proton transfer of alizarin investigated by femtosecond stimulated Raman spectroscopy. *Journal of Physical Chemistry B*. 2017;**121**:4129-4136. DOI: 10.1021/jp0155819
- [45] Peng CY, Shen JY, Chen YT, Wu PJ, Hung WY, Hu WP, et al. Optically triggered stepwise double-proton transfer in an intramolecular proton relay: A case study of 1,8-Dihydroxy-2-naphthaldehyde. *Journal of the American Chemical Society*. 2015;**137**:14349-14357. DOI: 10.1021/jacs.5b08562
- [46] Liu X, Zhao J, Zheng Y. Insight into the excited-state double proton transfer mechanisms of doxorubicin in acetonitrile solvent. *RSC Advances*. 2017;**7**:51318-51323. DOI: 10.1039/C7RA08945G
- [47] Martens WN, Frost RL, Kristof J, Klopogge JT. Raman spectroscopy of dimethyl sulphoxide and deuterated dimethyl sulphoxide at 298 and 77 K. *Journal of Raman Spectroscopy*. 2002;**33**:84-91. DOI: 10.1002/jrs.827
- [48] Singh S, Krueger PJ. Raman spectral studies of aqueous solutions of non-electrolytes: Dimethylsulfoxide, acetone and acetonitrile. *Journal of Raman Spectroscopy*. 1982;**13**:178-188. DOI: 10.1002/jrs.1250130214
- [49] Berg M. Viscoelastic continuum model of nonpolar solvation. 1. Implications for multiple time scales in liquid dynamics. *Journal of Physical Chemistry A*. 1998;**102**:17-30. DOI: 10.1021/jp9722061
- [50] Stephens MD, Saven JG, Skinner JL. Molecular theory of electronic spectroscopy in nonpolar fluids: Ultrafast solvation dynamics and absorption and emission line shapes. *Journal of Chemical Physics*. 1997;**106**:2129-2144. DOI: 10.1063/1.473144
- [51] Rosspeintner A, Lang B, Vauthey E. Ultrafast photochemistry in liquids. *Annual Review of Physical Chemistry*. 2013;**64**:247-271. DOI: 10.1146/annurev-physchem-040412-110146
- [52] Deák JC, Pang Y, Sechler TD, Wang Z, Dlott DD. Vibrational energy transfer across a reverse micelle surfactant layer. *Science*. 2004;**306**:473-476. DOI: 10.1126/science.1102074
- [53] Dlott DD. Vibrational energy redistribution in polyatomic liquids: 3D infrared-Raman spectroscopy. *Chemical Physics*. 2001;**266**:149-166. DOI: 10.1016/S0301-0104(01)00225-7